

In Vitro Pharmacokinetic Characterization of Mulberroside A, the Main Polyhydroxylated Stilbene in Mulberry (*Morus alba* L.), and Its Bacterial Metabolite Oxyresveratrol in Traditional Oral Use

Mei Mei,[†] Jian-Qing Ruan,[†] Wen-Jin Wu,[†] Rui-Na Zhou,[†] Jacky Pui-Cheong Lei,[§] Hai-Yu Zhao,[†] Ru Yan,^{*,†} and Yi-Tao Wang^{†,‡}

[†]State Key Laboratory of Quality Research in Chinese Medicine, Institute of Chinese Medical Sciences, University of Macau, Taipa, Macao, China

[‡]School of Chinese Materia Medica, Beijing University of Chinese Medicine, Beijing, China

[§]Clinical Laboratory, Kiang Wu Hospital, Estrada do Repouso, Macau, China

ABSTRACT: Mulberroside A (MulA) is one of the main bioactive constituents in mulberry (*Morus alba* L.). This study examined the determining factors for previously reported oral pharmacokinetic profiles of MulA and its bacterial metabolite oxyresveratrol (OXY) on in vitro models. When incubated anaerobically with intestinal bacteria, MulA underwent rapid deglycosylation and generated two monoglucosides and its aglycone OXY sequentially. MulA exhibited a poor permeability and predominantly traversed Caco-2 cells via passive diffusion; yet, the permeation of OXY across Caco-2 cells was much more rapid and involved efflux (both *p*-glycoprotein and MRPs)-mediated mechanisms. Moreover, OXY underwent extensive hepatic glucuronidation; yet, the parent MulA was kept intact in liver subcellular preparations. There was insignificant species difference in intestinal bacterial conversion of MulA and the extent of OXY hepatic glucuronidation between humans and rats, while OXY exhibited a distinct positional preference of glucuronidation in the two species. Overall, these findings revealed a key role of intestinal bacterial conversion in absorption and systemic exposure of MulA and its resultant bacterial metabolite OXY in oral route in humans and rats and warranted further investigational emphasis on OXY and its hepatic metabolites for understanding the benefits of mulberry.

KEYWORDS: *Morus alba* L., mulberroside A, oxyresveratrol, hydroxystilbenes, intestinal bacteria, deglycosylation, permeability, glucuronidation

■ INTRODUCTION

Morus alba L. (mulberry) is a well-known plant that is widely cultivated in many countries for different purposes, including the leaves as feed for silkworms; fruits as dietary supplements; and leaves, fruits, twigs, and root bark for medicinal uses in some Asian countries.¹ Modern biological evaluations have revealed health-promoting effects of mulberry, including antibacterial, hypolipidemic, antioxidant, antityrosinase, neuroprotective, nephroprotective, hypoglycemic, antidiabetic, and adaptogenic activities, etc.,^{2–5} supporting its attractive perspectives for health promotion.

Mulberry is rich in polyphenols, alkaloids, flavonoids, and anthocyanins, which have been suggested to be responsible for its health benefits. *trans*-Hydroxystilbenes are a group of polyphenolic compounds naturally occurring in large amounts in mulberry.⁶ Mulberroside A (MulA, Figure 1) is reported to be the main polyhydroxylated stilbene of the water extract of the root bark of mulberry (~0.8% of crude drug).⁷ It has exhibited a wide beneficial profile^{8,9} and thereby is considered as the main active component of mulberry in a conventional oral route of aqueous decoctions.

MulA exhibited a poor oral bioavailability (<1%) in the rat.¹⁰ Zhaxi and co-workers found oxyresveratrol (OXY) and two OXY monoglycosides in rat gastrointestinal (GI) contents and feces after oral administration of MulA.¹¹ The main forms detected in rat plasma, bile, and urine were OXY and OXY

conjugates (glucuronidate and/or sulfate), which accounted for ~50% of the oral dose of MulA.^{10,11} These findings suggest a rapid conversion of MulA to OXY in the rat GI tract after oral dosing, which may enable OXY as the main form that has been absorbed and subjected to extensive hepatic conversions before entering the systemic circulation to elicit activities. Thus, in the present study, the metabolic stability of MulA in the gut lumen prior to its absorption, trans-epithelial permeability, and hepatic metabolic stability of MulA and OXY were examined in vitro, for the first time, to unravel the determinant factors for systematic exposure of MulA. As a polyphenolic compound, the stability of MulA in different pH matrices was also determined. The findings may shed light on pharmacokinetic basis under health benefits of MulA and mulberry and respective contributions of MulA and its resultant OXY. In addition, so far, the biological activities and in vivo pharmacokinetic profile of MulA have been characterized with rats; whether MulA exhibits a distinct pharmacokinetic profile in humans due to species difference in gut microbiota^{12,13} and hepatic drug-metabolizing enzymes^{14,15} remains to be addressed.

Received: July 22, 2011

Revised: December 22, 2011

Accepted: December 22, 2011

Published: December 22, 2011

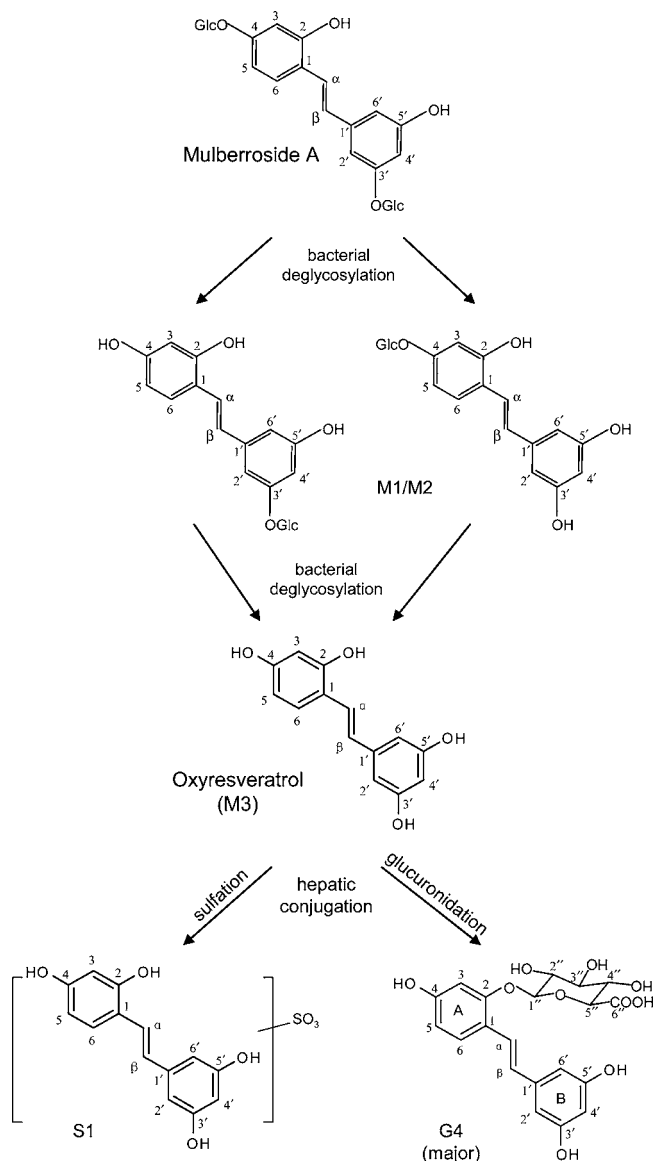


Figure 1. Chemical structures of MulA and oxyresveratrol and their proposed metabolic changes in humans.

Therefore, the present study aimed to (1) characterize the chemical and metabolic stability of MulA in gut lumen prior to absorption, (2) compare the permeability of MulA and OXY across intestinal epithelia on a Caco-2 cell monolayer, (3) examine the hepatic metabolic stability of MulA and OXY in rat and human livers, and (4) identify the species difference in bacterial conversion and hepatic metabolism, if any.

MATERIALS AND METHODS

Materials. All chemicals were from Sigma-Aldrich (St. Louis, MO) unless otherwise claimed. MulA and OXY (purities >98%) were supplied by Kuiqing Co., Ltd. (Tianjin, China). Kaempferol (purity >98%) was from the National Institute for the Control of Pharmaceutical and Biological Products (Beijing, China) and was utilized as an internal standard (IS). BBL Brain Heart Infusion (BHI) medium, GasPak EZ anaerobe container system with indicator, and a GasPak EZ large incubation container were purchased from Becton Dickinson (Franklin Lakes, NJ). L-Cystine was from Research Organics, Inc. (Cleveland, OH). Trishydroxymethylaminomethane was obtained from USB Corp. (Cleveland, OH). Acetic acid and trichloroacetic acid were analytical grade from UNI-CHEM Chemical

Reagent Co., Ltd. (Wuxi, China) and Damao Co., Ltd. (Tianjin, China), respectively. Methanol, *n*-butanol, and formic acid were high-performance liquid chromatography (HPLC)-grade from Merck (Darmstadt, Germany). Dulbecco's modified Eagle's medium (DMEM), fetal bovine serum (FBS), 0.25% trypsin-EDTA, penicillin–streptomycin solution, and nonessential amino acids were purchased from GibcoBRL Life & Technologies (Grand Island, NY). Deionized water was obtained using a Milli-Q purification system (Millipore, Bedford, MA). GF/F glass fiber filters were obtained from Whatman (Brentford, United Kingdom). 12-Well transwell plates (0.4 μm pore size, 1.12 cm^2 , polycarbonate filter) were supplied by Corning Costar Co. (Cambridge, MA).

Caco-2 cells were obtained from the American Type Culture Collection (Rockville, MD). Pooled human liver microsomes (HLMs) and S9 were purchased from BD Biosciences (Billerica, MA). The pools of rat liver S9 and microsomes (RLMs) were prepared from 30 healthy Sprague–Dawley rats (male, 250–300 g) by differential centrifugation according to a standard procedure. The protein content of each preparation was determined by Lowry's method.¹⁶ All preparations were stored at $-80\text{ }^\circ\text{C}$ until use.

Preparation of Human and Rat Intestinal Bacteria. The culture medium was 100 mL autoclaved BHI medium (3.7 g/100 mL) supplemented with 0.05 mg of vitamin K1, 0.5 mg of hemin bovine, and 50 mg of L-cystine. Human and rat intestinal bacterial solutions were prepared according to our previous report¹⁷ with minor modifications. Briefly, fresh human fecal samples were collected from six healthy Chinese volunteers (20–30 year, two males and four females) from the Institute of Chinese Medical Sciences, University of Macau, and 1 g of each was pooled and mixed with 60 mL of culture medium. The resultant fecal suspension was centrifuged at 200g for 5 min. The precipitate was resuspended and centrifuged at 5000g for 30 min. After the supernatant was decanted, the precipitate was resuspended with BHI medium to produce human intestinal microflora solution (0.5 mg mL^{-1} bacteria). Fresh rat fecal samples were collected from eight male Sprague–Dawley rats (200–250 g), and 0.6 g of each was pooled together and treated as described above to obtain rat intestinal microflora solution (0.5 mg mL^{-1} bacteria). All fecal samples were collected and processed according to a protocol approved by the Panel on Research Ethics of the Research & Development Administration Office, University of Macau.

Stability of MulA in Matrices at Different pH. The stability of MulA under the variable pH environment along the GI tract was examined by incubating MulA at 37 $^\circ\text{C}$ with simulated gastric fluid (pH 1.5)¹⁸ and HBSS buffer (pH 7.4, 6.8 and 6.0), for up to 1 and 2 h, respectively. To aid structural identification of MulA metabolites generated from deglycosylation by intestinal bacteria, MulA (10 mM in DMSO) was dissolved in deionized water containing 5% (v/v) 1 M HCl (MulA final concentration, 100 μM). The mixed solution was kept at 90 $^\circ\text{C}$ for 6 h and then extracted once with 1 mL of water-saturated 1-butanol. The organic layer was collected and evaporated under N_2 at 37 $^\circ\text{C}$. The residue was reconstituted with 100 μL of methanol, and then, an aliquot (10 μL) was subjected to HPLC–ultraviolet (UV) or HPLC–mass spectrometry (MS) analysis.

Metabolism of MulA by Human and Rat Intestinal Bacteria.

The incubation system contains 25 μL of intestinal microflora solution and 5 μL of MulA in DMSO and BHI medium in a total volume of 500 μL (MulA final concentration, 100 μM). The reaction system was anaerobically incubated at 37 $^\circ\text{C}$ in a GasPak EZ Anaerobe Pouch system for different time intervals (0, 0.17, 0.33, 0.5, 0.75, 1, 1.5, 2, 2.5, 3, 3.5, and 4 h). Zero-minute incubations or parallel reactions without microflora or MulA served as controls. At the end of reactions, 5 μL of the internal standard kaempferol (1 mg mL^{-1} in DMSO) was added and thoroughly vortexed to mix, followed by immediate addition of 1 mL of ice-cold water-saturated 1-butanol. The resultant mixture was centrifuged at 15000g for 10 min, and the supernatant was evaporated under N_2 at 37 $^\circ\text{C}$. The residue was processed and analyzed in the same manner as described above.

Cell Culture. Caco-2 cells at passages from 30 to 40 were used for the experiment. The cells were seeded on 12-well plates and cultured under conditions as previously reported.¹⁷ The integrity of the

monolayer was monitored by measuring the transepithelial electrical resistance (TEER) at 37 °C with an epithelial voltohmmeter (World Precision instruments, Inc., FL) before and after the transport study. Only Caco-2 monolayers with TEER above 300 Ω cm² were adopted in the transport study. The functionality of Caco-2 monolayers was validated by measuring P_{app} values of the paracellular marker lucifer yellow, the transcellular marker propranolol, and the P-glycoprotein (P-gp) probe substrate rhodamine 123. Lucifer yellow exhibited P_{app} values of $0.183 \pm 0.099 \times 10^{-6}$ cm s⁻¹ and propranolol $12.250 \pm 2.590 \times 10^{-6}$ cm s⁻¹. Moreover, rhodamine 123 exhibited substantial polarized transport, and the efflux ratio was 35.7. Thus, the Caco-2 monolayer possesses normal paracellular, transcellular, and efflux transport functions.

Sulforhodamine B Toxicity Assay. The sulforhodamine B assay¹⁹ was performed to determine the cytotoxicity of MulA and OXY prior to the transport study. Preliminary data indicated that MulA was stable, while OXY was pH-sensitive and only kept intact (>95% of added amount) within 2 h when the pH of the medium was lowered to 6.0 (data not shown). Thus, the following cytotoxicity assay and the transport study were carried out in HBSS buffer at pH 7.4 for MulA and pH 6.0 for OXY, respectively. Caco-2 cells were seeded at a density of 1×10^4 /well into 96-well plates and cultured as described above. After 24 h of incubation, the medium was replaced with 200 μ L of HBSS buffer (control), HBSS containing different amounts of MulA (final concentrations, 3–200 μ M) at pH 7.4, or OXY (final concentrations, 6–400 μ M) at pH 6.0. After exposure to test compound or HBSS alone at 37 °C for 4 h, the cells were fixed with ice-cold trichloroacetic acid (final concentration, 10% v/v) at 4 °C for 1 h. Then, the cell plates were washed with deionized water and allowed to dry at ambient temperature. Afterward, the cells were stained with sulforhodamine B solution (4 mg mL⁻¹, 100 μ L/well) for 30 min at room temperature, then rinsed with 1% acetic acid for three times to remove unbound dye, and air-dried. The sulforhodamine B formed was solubilized with 200 μ L of tris(hydroxymethyl)aminomethane (100 mM), and the absorbance was measured at a wavelength of 490 nm using spectrophotometry.

Transport Studies of MulA and OXY. After 21 days of culture, the Caco-2 monolayers were rinsed twice with HBSS and preincubated in HBSS at 37 °C for 30 min. In the absorptive transport study, 0.5 mL of HBSS solution containing test compound was loaded at the apical (A) side (donor chamber) and 1.5 mL of blank HBSS placed at the basolateral (B) side (receiver chamber). In the secretory transport study, 1.5 mL of the HBSS-containing test compound was added at the B side (donor chamber), and 0.5 mL of blank HBSS was placed at the A side (receiver chamber). Aliquots (100 μ L) were taken from the receiver chamber at appropriate time intervals (MulA: 0, 1, 1.5, 2, and 2.5 h; OXY: 0, 0.25, 0.5, 0.75, 1, and 1.25 h). After each sampling, 100 μ L of HBSS was supplemented to the receiver chamber to maintain a constant volume. At the end of the experiment, samples were also withdrawn from the donor chamber to calculate the recovery. Samples collected from the MulA study were directly injected into an HPLC instrument. Because of the instability of OXY in HBSS, samples collected from the transport study of OXY were mixed with 2 μ L of kaempferol (0.2 mg mL⁻¹ in DMSO), extracted once with 1 mL of ice-cold 1-butanol, and then centrifuged at 5000g for 5 min. The organic layer was collected and evaporated under N₂ at 37 °C, and the residue was reconstituted with 100 μ L of methanol/water (50/50, v/v) before subjecting it to HPLC-UV or HPLC-MS analysis.

The involvement of efflux transporters in OXY transport was determined by adding either of the following inhibitors in both sides and incubated with the cell monolayers for 30 min at 37 °C before adding OXY: 100 μ M verapamil (the P-gp inhibitor) and 10 μ M indomethacin [the multidrug resistance-associated proteins (MRPs) inhibitor].

To determine the extent of cell accumulation of test compound, Caco-2 monolayers were removed from transwell plates at the end of the transport study, rinsed twice with deionized water, and then sonicated in methanol for 30 min. The resultant methanol solution was evaporated under N₂, and the residue was reconstituted with 100 μ L of HBSS prior to HPLC-UV analysis.

Metabolic Studies of MulA and OXY in Human and Rat Hepatic Subcellular Fractions. Metabolic profiles of MulA and OXY were characterized with human and rat liver subcellular fractions in a total of 200 μ L reaction solution containing MulA or OXY (final concentration, 100 μ M) under the following different conditions:

Phase I reaction: 0.8 mg/mL liver microsomes, NADPH-regenerating system [4 mM MgCl₂, 1 mM NADP⁺, 1 mM glucose-6-phosphate, and 1 U mL⁻¹ glucose-6-phosphate dehydrogenase (G-6-PD) in 100 mM potassium phosphate buffer (pH 7.4)];

Glucuronidation: 0.8 mg mL⁻¹ liver microsomes, 8 mM MgCl₂, 2 mM uridine diphosphate glucuronic acid (UDPGA), and 25 μ g of alamethicin in 50 mM Tris-HCl (pH 7.4);

Sulfation: 0.8 mg mL⁻¹ liver S9, 5 mM MgCl₂, 8 mM DTT, 0.0625% BSA, and 200 μ M 3'-phosphoadenosine 5'-phosphosulfate (PAPS) in 50 mM Tris-HCl (pH 7.4).

All reactions were preincubated at 37 °C for 5 min and initiated by adding the cofactor (G-6-PD, UDPGA, or PAPS, respectively) and kept at 37 °C for 10 min (glucuronidation) or 1 h (phase I and sulfation). Reactions without the cofactors served as controls. All of the experiments were performed in duplicate. Reactions were terminated by adding 100 μ L of ice cold methanol. After centrifugation at 15000g for 10 min at 4 °C, the supernatants were subjected to HPLC-UV or HPLC-MS analysis.

Calibration Curves of MulA and OXY for in Vitro Studies.

MulA and OXY stock solutions were prepared and diluted to different concentrations with DMSO. For the transport study, the serial solutions of MulA were diluted with HBSS at pH 7.4 (final 1% DMSO, v/v) to 0.39–200 μ M and applied to HPLC-UV analysis directly. Calibration curves of MulA were constructed by plotting the peak area of MulA as a function of MulA concentration. The serial solutions of OXY were diluted with HBSS at pH 6.0 (final 1% DMSO, v/v) to 0.39–400 μ M. These samples were then mixed with kaempferol (final concentration, 4 μ g/mL) and processed as described above. Calibration curves of OXY were constructed by plotting the peak area ratio of OXY to the internal standard as a function of OXY concentration.

For the bacterial conversion study, the serial solutions of MulA or OXY were spiked with BHI medium and rat bacterial solution (final concentrations: DMSO, 1% v/v; MulA, 0.39–100 μ M; and OXY, 0.39–100 μ M). After the addition of 5 μ L of kaempferol (final concentration, 10 μ g/mL) as an internal standard, the sample was extracted with 1-butanol and processed as described above before it was subjected to HPLC analysis. The calibration curves were constructed by plotting the peak area ratio of the analyte to the internal standard as a function of the concentration of the analyte.

For hepatic biotransformation study, the serial solutions of MulA or OXY were spiked with the in vitro hepatic microsomal incubation system in the absence of the NADPH-regenerating system with the concentration ranges of the analytes the same as the bacterial conversion study. The mixtures were then mixed with the internal standard (final concentration, 10 μ g/mL), treated with 1 volume of ice-cold methanol, and centrifuged to remove proteins. The resultant supernatant was subjected to HPLC-UV or HPLC-MS analysis directly. Calibration curves were obtained by plotting the peak area ratio of the analyte to the internal standard as a function of the concentration of the analyte.

HPLC-UV Analysis. All samples were analyzed on an Agilent series 1200 (Agilent Technologies, Palo Alto, CA) liquid chromatography that equipped with a vacuum degasser, a binary pump, an autosampler, and a diode array detector (DAD) system and operated with an Agilent ChemStation B 3.0 software. An Alltech Alltima C18 column (250 mm \times 4.6 mm, 5 μ m) was used for separation at 25 °C. The mobile phase consisted of 0.1% aqueous formic acid (A) and methanol (B) and eluted at 1 mL/min with a linear gradient increasing from 5 to 100% B within 38 min. The UV spectra were obtained over 210–380 nm. MulA, OXY, the internal standard kaempferol, and all other metabolites were monitored at 320 nm. The injection volumes were 10 μ L of samples from stability test and intestinal bacterial conversion

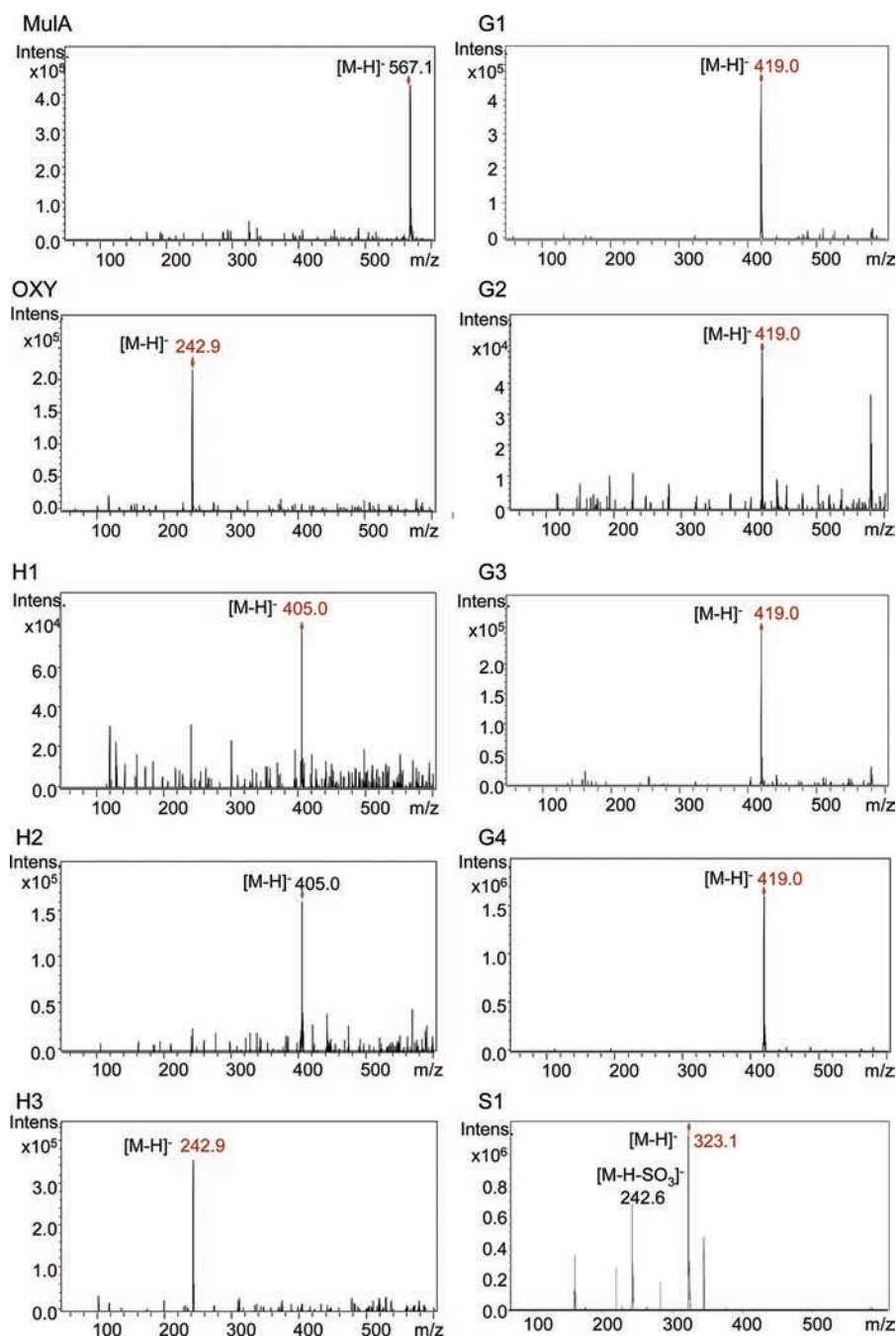


Figure 2. MS¹ spectra of Mula, OXY, metabolites (H1–H3) of Mula formed by human intestinal bacteria, and hepatic metabolites (G1–G4, S1) of OXY.

studies and 70 μL of samples from the transport study or hepatic metabolic study.

HPLC-MS Analysis. MS was performed on an LC/MSD Ion Trap system (Agilent Technologies) consisting of an Agilent 1100 series HPLC system and an ion-trap mass spectrometer. HPLC separation was conducted as described above. The MS was operated in electrospray ionization-negative ion mode and controlled by an Agilent ChemStation software. ESI-MS analytical conditions were as follows: dry gas, N₂ (8 L/min); dry temperature, 350 °C; nebulizer pressure, 40 psi; capillary voltage, –3500 V; and scan range, m/z 50–600. ESI-MS/MS analysis was performed in negative ion mode under the following conditions: separation width, 4; fragment amplification, 1.5; and the scan range, m/z 50–600.

Nuclear Magnetic Resonance (NMR) Analysis of G4. G4, the major metabolite of OXY in HLMs, was prepared from a scale-up

reaction with HLMs and isolated using preparative HPLC. NMR spectra [¹H, ¹³C, heteronuclear single quantum coherence, heteronuclear multiple bond correlation, rotating frame Overhauser effect spectroscopy, and nuclear Overhauser effect spectroscopy (NOESY)] of G4 were recorded on a Bruker AV-600 (Bruker, Newark, Germany), using TMS as the internal standard. Chemical shifts were expressed in δ , and coupling constants (J) were reported in Hertz (Hz).

Data Analysis. The apparent permeability coefficients (P_{app}) of test compound from the apical side to the basolateral side ($P_{\text{appA} \rightarrow \text{B}}$) or from the basolateral side to the apical side ($P_{\text{appB} \rightarrow \text{A}}$) in the bidirectional transport study were calculated using the following equation:

$$P_{\text{app}} = (dC/dt \times V)/(C_0 \times A)$$

where dC/dt is the rate of the test compound appearing in the receiver chamber, V is the volume of the solution in the receiver chamber, C_0 is the initial concentration of the compound added in the donor chamber, and A is the cell monolayer surface area. An efflux ratio ($P_{appB \rightarrow A}/P_{appA \rightarrow B}$) > 2 was adopted when determining whether efflux transporter(s) was involved.

The area under peak area ratio–time curve (AUP) of MulA metabolites formed from intestinal bacterial incubations was calculated by linear trapezoidal method using WinNonlin 5.2.1 software (Pharsight, United States) and used for comparison of the relative amounts between metabolites within the same species or the same metabolite between humans and rats.

All data were expressed as means \pm standard deviations (SD). The apparent permeability coefficient (P_{app}) values of test compound were compared between absorptive direction ($P_{appA \rightarrow B}$) and secretory direction ($P_{appB \rightarrow A}$) and between inhibitor treated and untreated groups using unpaired Student's t test. A $P < 0.05$ value was deemed significant for all tests.

RESULTS

HPLC-UV and HPLC-MS Analysis of MulA and OXY.

Under the developed analytical conditions, MulA and OXY were eluted at 16.0 and 21.7 min, respectively. Both analytes showed good linearity within tested concentration ranges in different in vitro systems: transport study, $Y = 21.81X - 12.38$ (MulA) and $Y = 0.608X + 2.686$ (OXY); bacterial conversion study, $Y = 0.027X + 0.004$ (MulA) and $Y = 0.052X - 0.026$; and hepatic metabolism study, $Y = 0.032X + 0.002$ (MulA) and $Y = 0.059X + 0.021$ (OXY); $r^2 > 0.99$ in all cases.

The MS¹ data of MulA and OXY standards are shown in Figure 2. MS¹ of MulA showed a pseudo molecular ion ($[M - H]^-$) at m/z 567, which produced product ions at m/z 405 and m/z 243 in the MS² spectrum, corresponding to the loss of one and two glucose molecules from MulA, respectively. OXY had a $[M - H]^-$ ion at m/z 243 and generated characteristic ions at m/z 225 ($[M - H - H_2O]^-$), m/z 199 ($[M - H - CH_2=CH-OH]^-$), m/z 185, and m/z 97 at comparable abundance in its MS² spectrum.

Stability of MulA in Matrices at Different pH. MulA showed high stability at all tested pH conditions (data not shown). When incubated with simulated gastric fluid, MulA kept intact over 1 h of incubation. While in 1 M HCl at 90 °C, MulA showed a rapid degradation, and three peaks (M1, M2, and M3) were observed. The three products were eluted at retention times of 17.9 (M1), 18.4 (M2), and 21.7 min (M3), sequentially (Figure 3A).

MS¹ spectra of both M1 and M2 showed a pseudomolecular ion ($[M - H]^-$) at m/z 405, which was 162 mass units less than that of MulA (m/z 567), corresponding to the loss of one glucose molecule (Figure 2). The MS² of m/z 405 of both metabolites yielded the predominant fragment ion at m/z 243, indicating the loss of the other glucose moiety. Thus, M1 and M2 should be monoglucosides of OXY formed from deglycosylation of MulA at either C-3' or C-4. M3 showed an identical retention time and UV and mass spectra to those of OXY and thus was unambiguously identified as OXY formed from sequential loss of two glucoses from MulA.

Metabolism of MulA by Human and Rat Intestinal Bacteria. When incubated anaerobically with human intestinal bacteria, MulA decreased rapidly with time and was not detectable at 3 h after incubation (Figure 4A). Three additional peaks that showed retention times and UV and MS spectra identical to those of M1–M3, respectively, were observed and confirmed to be metabolites of MulA when compared with

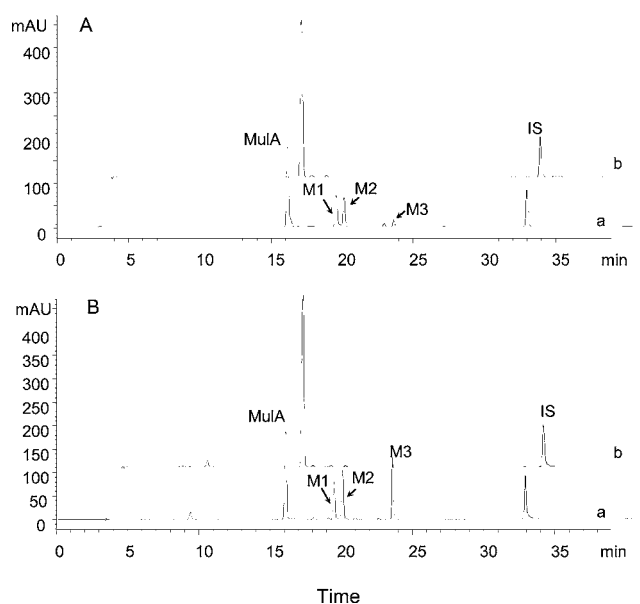


Figure 3. Typical HPLC chromatograms of incubations of MulA with HCl (A) and human intestinal bacteria (B). (a) Reaction with bacteria or HCl and (b) control reaction without bacteria or HCl.

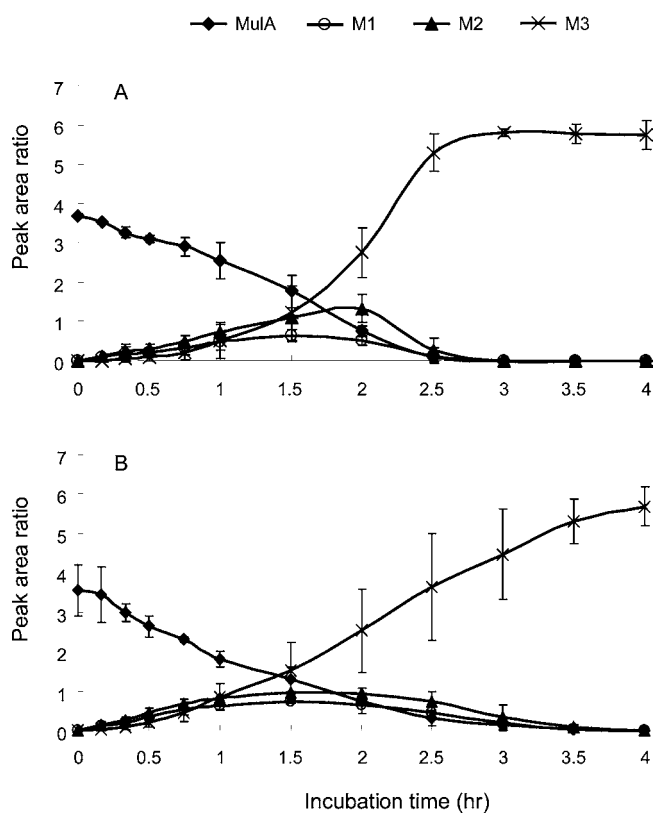


Figure 4. Time courses of MulA metabolism by human (A) and rat (B) intestinal bacteria. Data were presented as means \pm SDs, $n = 3$.

controls (Figure 3B). Similarly, in rat intestinal bacteria, MulA also showed a rapid elimination and gave the same three metabolites according to their retention times and UV and MS spectral data. Thus, the metabolites of MulA formed by intestinal bacteria from humans and rats were the same as the three products from acidic treatment of MulA. M1 and M2 were tentatively assigned as OXY monoglucosides with one as 4-O- β -

D-glucopyranoside and the other as 3'-O- β -D-glucopyranoside and M3 unambiguously as OXY (Figure 1).

Time Course of Mula Metabolism by Human and Rat Intestinal Bacteria. As shown in Figure 4, Mula exhibited a rapid linear elimination ($y = -1.36x + 3.76$, $r^2 = 0.98$) and disappeared within 3 h with an average velocity of elimination at $0.016 \mu\text{mol h}^{-1}$ when incubated with human intestinal bacteria (Figure 4A). The two monoglucosides of OXY, M1 and M2, increased with time, reached their maximum at 1.5–2 h, and then were not detectable within 1 h. The AUP value of M2, which was calculated on the basis of peak area ratio of each metabolite to the internal standard over 4 h of incubation, was around two times that of M1 (1.89 ± 0.15 vs 1.00 ± 0.43). The increase of OXY was slow within the first 1.5 h and then increased much faster before reaching a plateau in another hour.

In the case of rat intestinal bacteria, metabolic conversion of Mula occurred linearly yet slightly slower ($y = -1.07x + 3.23$, $r^2 = 0.94$) than that in human intestinal bacteria (Figure 4B). It took 4 h to deplete Mula, and the overall elimination rate was $0.013 \mu\text{mol h}^{-1}$. The rates of M1 and M2 increase within first 2 h were similar to the increase of the two metabolites in human intestinal bacteria, respectively; yet, the elimination of M1 and M2 in rat intestinal bacteria was slightly slower, suggesting a slower deglycosylation of the OXY monoglucosides by microbiota from rats than those from humans. As a consequence, a slower increase of OXY was observed with the maximum appeared at 4 h. The average velocity of OXY formation by rat was around half of that formed by human as judged based on the slopes of OXY formation curves over 1.5–2.5 h. Similarly, the AUP of M1 (1.52 ± 0.05) was smaller than that of M2 (2.17 ± 0.28).

Transport of Mula and OXY across Caco-2 Monolayer. Sulforhodamine B toxicity assays revealed nontoxicity of Mula and OXY toward Caco-2 monolayers within 4 h over the respective concentration range tested. Therefore, the transport studies were carried out over 25–200 (Mula) and 50–400 μM (OXY).

The P_{app} values of Mula and OXY obtained from bidirectional transport studies are summarized in Table 1.

Table 1. Apparent Permeability Coefficients (P_{app}) of Mula and Oxyresveratrol at Different Concentrations on a Caco-2 Cell Model^a

compd	concn (μM)	cm s^{-1}		efflux ratio
		$P_{\text{app A}\rightarrow\text{B}}, \times 10^{-7}$	$P_{\text{app B}\rightarrow\text{A}}, \times 10^{-7}$	
Mula	50	1.17 ± 0.50	1.85 ± 0.29	1.59
	100	1.08 ± 0.32	1.40 ± 0.72	1.30
	200	1.29 ± 0.65	1.63 ± 0.51	1.49
OXY	200	8.49 ± 0.23	$35.87 \pm 3.70^{**}$	4.22
	300	12.50 ± 1.13	$45.48 \pm 3.45^{**}$	3.64
	400	16.29 ± 3.3	$50.43 \pm 3.75^{**}$	3.10
	200 (verapamil 100 μM)	$22.48 \pm 4.79^{\#\#}$	$28.41 \pm 2.01^{\#}$	1.28
	200 (indomethacin 10 μM)	$11.19 \pm 1.33^{\#}$	$26.01 \pm 4.34^{**\#}$	2.32

^a** $p < 0.01$ as compared with the corresponding $P_{\text{app A}\rightarrow\text{B}}$ value; $\#p < 0.05$, $\#\#p < 0.01$ as compared with the corresponding $P_{\text{app A}\rightarrow\text{B}}$ or $P_{\text{app B}\rightarrow\text{A}}$ value for 200 μM OXY in the absence of inhibitors.

Mula was not detectable at receiver chambers at 25 μM in both directions, and OXY was not detectable at receiver chambers at 50 and 100 μM in the absorptive direction; thus, the efflux ratios were not available for these concentrations and data not shown in Table 1.

Mula exhibited very low P_{app} values ($\times 10^{-7} \text{ cm s}^{-1}$) in both directions, indicating a poor oral absorption in the human body. The bidirectional P_{app} values of Mula obtained for different concentrations were similar, indicating a dose-independent transport. Furthermore, efflux ratios were all less than 2, suggesting that passive diffusion dominate Mula transport across Caco-2 monolayers.

As has been expected, the aglycone OXY exhibited P_{app} values ($\times 10^{-6} \text{ cm s}^{-1}$) that were 1 order of magnitude higher than that of Mula. Different from that observed with Mula, OXY exhibited higher transport in the secretory direction than the absorptive direction over the concentration range tested (Table 1). Moreover, the efflux ratio of OXY was 4.22 at 200 μM and increased inversely with dose, suggesting that OXY might be the substrate of efflux transporter(s). At 200 μM OXY, the P-gp inhibitor verapamil abolished the directional preference of OXY transport with an efflux ratio of 1.27, the MRPs inhibitor indomethacin substantially diminished the polarized transport, and the efflux ratio was 2.32.

Both Mula and OXY showed high recovery from the transport study. No Mula was detected in Caco-2 cells, and the amount of OXY trapped in Caco-2 cells was negligible ($<1\%$). No additional peak was detected in cells or culture media during the permeation of OXY or Mula across the Caco-2 cell monolayers.

In Vitro Hepatic Metabolism of Mula and OXY. When incubated with liver subcellular fractions of humans or rats for 1 h, the recovery of Mula was $>96\%$ in the presence of the corresponding cofactor. Furthermore, HPLC-MS analysis also revealed no metabolites of Mula (data not shown). OXY exhibited a high ($>95\%$) recovery from reactions with liver microsomes from both species in the absence/presence of a NADPH-regenerating system. HPLC-MS analysis also revealed no additional peaks (data not shown). In contrast, four additional peaks, namely, G1, G2, G3, and G4, were observed in the 1 h reaction with HLMs or RLMs as compared to control reactions (Figure 5A,B). There were comparable OXY loss (HLMs, 90%; and RLMs, 97%) over 10 min in the presence of UDPGA with the average velocity of OXY elimination of 11.4 and 12.1 $\text{nmol min}^{-1} \text{ mg}^{-1} \text{ protein}$, respectively, indicating an extensive glucuronidation of OXY in both species. However, the formation of G4 was highest in HLMs; yet, G3 was the most predominant metabolite of RLMs. When compared with the peak area values, the amount of G4 formed in HLMs was seven times that in RLMs, and G3 formation in RLMs was 20 times that in HLMs. In hepatic S9, minor sulfation was evidenced by OXY loss over 1 h of incubation (human, 10%; and rat, 15%) and the simultaneous appearance of one additional peak, namely, S1 (Figure 5C) in the presence of PAPS. The average velocity of OXY elimination via sulfation was 0.19 (human) versus 0.31 (rat) $\text{nmol min}^{-1} \text{ mg}^{-1} \text{ protein}$.

The mass spectra of G1–G4 and S1 are shown in Figure 3. G1–G4 all exhibited pseudomolecular ions $[\text{M} - \text{H}]^{-}$ at m/z 419 in their mass spectra, corresponding to a molecular mass of 420 Da, which was 176 mass units (equal to one glucuronic acid molecule) higher than the molecular mass of OXY ($[\text{M} - \text{H}]^{-}$ at m/z 243). Thus, the four metabolites were all monoglucuronidates of OXY. Their relative amounts, as

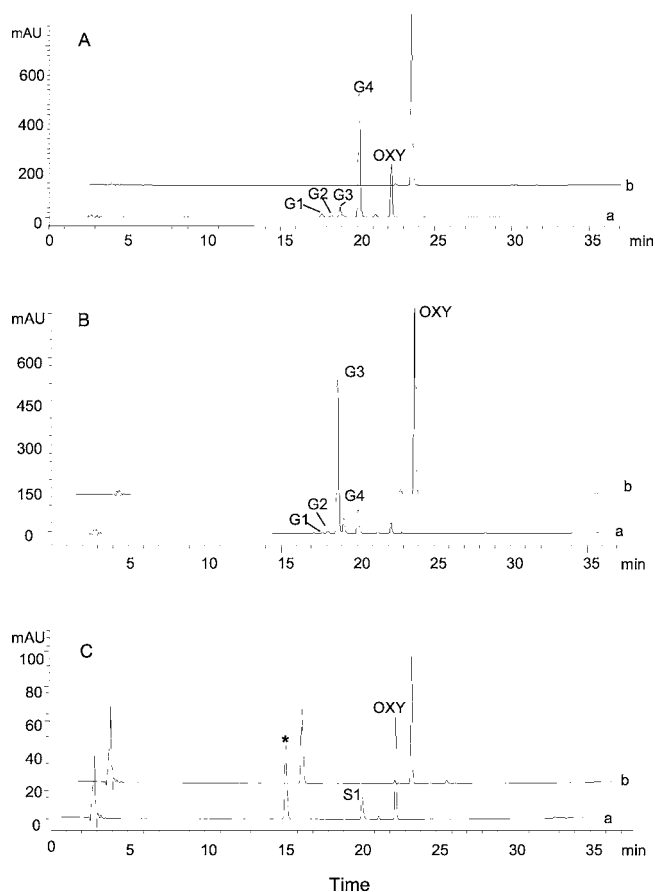


Figure 5. Typical HPLC chromatograms of incubations of OXY with liver microsomes of human (A) and rat (B) for 10 min and human S9 (C) for 60 min. (a) Reaction in the presence of cofactor and (b) reaction without cofactor. *, impurity in the incubation system.

calculated based on the percentage of the peak area of each to the sum of the four, were in the following descending order: human: G4 (92.7%), G3 (4.0%), G1 (2.3%), and G2 (1.0%); rat: G3 (85.1%), G4 (13.2%), G2 (1.3%), and G1 (0.4%). The mass spectrum of S1 revealed a pseudomolecular ion at m/z 323 and a characteristic fragment ion at m/z 243 ($[M - H - SO_3]^-$) (Figure 3), suggesting a monosulfated metabolite.

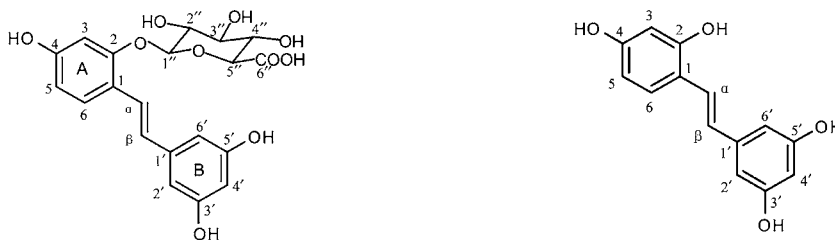
The 1H NMR spectrum of G4 showed signals due to *trans*-olefinic protons at $\delta = 7.31$ (1H, d, $J = 16.5$ Hz, H- α) and 6.80 (1H, d, $J = 16.5$ Hz, H- β), as well as proton signals belonging to two independent aromatic rings (Table 2). By comparison of the NMR data of G4 with those of OXY reported previously,¹¹ proton signals in ring A showed significant changes in especially the 1H NMR signal of C3-H (+0.22 ppm) and C5-H (+0.24 ppm) with a coupling constant of 2.3 Hz; yet, those in ring B were unaffected. The ^{13}C NMR spectrum of G4 exhibited significant downfield shifts of C2 (+1.4 ppm), C1 (+2.6 ppm), and C3 (+0.4 ppm) signals in comparison with OXY. Carbon signals (100.6, 73.2, 75.8, 71.4, 75.3, and 170.0 ppm) indicated the presence of a *D*-glucuronosyl moiety. The β -configuration of the glucuronide linkage was determined on the basis of the value of the characteristic coupling constant of the anomeric proton at $\delta = 4.95$ (1H, d, $J = 8.0$ Hz). The correlation signals between the anomeric proton at $\delta = 4.95$ and H-3 in the NOESY spectrum corroborated the linkage of glucuronide at C-2 of OXY. Taken together, G4 was unambiguously identified as OXY-2-*O*- β -*D*-glucuronosyl.

DISCUSSION

In daily life, most herbs or herbal products are used as food supplements and in forms of oral preparations. In the long history of traditional medicinal practice, medicinal herbs are usually prepared as decoctions and taken orally. Thus, when study nutritional or medicinal herbs on their traditional applications, emphasis should be put on the water-soluble constituents and their fates prior to entering systemic circulation to understand the pharmacokinetic basis under their *in vivo* benefits.

As one of the most abundant bioactive constituents in the water extract of mulberry root bark, MulA might be converted to OXY via deglycosylation in gut lumen as indicated by previous reports.^{9–11} Moreover, the existing *in vivo* pharmacokinetic data indicated the occurrence of phase II conjugation of OXY when a Mori Cortex extract, MulA, or OXY was administered orally to the rat.^{10,20} Recently, OXY has received more attention because of its structural similarity with resveratrol (3,5,4'-trihydroxy-*trans*-stilbene), the most important stilbene related to human health; yet, more potent bioactivities have been revealed.^{9,21–23} In consideration of the richness of MulA in mulberry and an increasing awareness of the benefits of its aglycone OXY, it is of great importance to understand the *in vivo* fates of MulA and its resultant OXY to estimate their respective contribution to the benefits of mulberry. Thus, in the present study, three steps that might be crucial for systematic exposures of MulA and OXY, including biotransformation by intestinal bacteria, transepithelial permeability, and hepatic metabolism, were examined. To our best knowledge, this is the first report on *in vitro* bacterial and hepatic metabolism and permeability evaluation of MulA and OXY. The results demonstrated a rapid hydrolysis of MulA to generate OXY in intestinal bacteria, a markedly higher permeability of OXY than MulA, and an extensive hepatic conversions of OXY. Among all of the factors examined, intestinal bacterial deglycosylation of MulA was similar between humans and rats and presented to be a determinant step for subsequent absorption and disposition of MulA and OXY and, consequently, their respective contribution to the benefits of mulberry. Although the extent of hepatic conjugation of the bacterial metabolite OXY was similar in liver microsomes of humans and rats, distinct positional preference of OXY hepatic glucuronidation may lead to a significant species difference in *in vivo* active forms and subsequent actions of MulA.

As expected, MulA underwent rapid stepwise deglycosylation in intestinal bacteria of humans and rats, indicating a similar low oral bioavailability of MulA in humans. The formation of the aglycone OXY was rapid, and its structure was unambiguously confirmed with standard OXY. The other two metabolites were tentatively determined based on the current mass data, and their structures were speculated as C-3' and C-4 monoglucosides of OXY, which were formed from removal of one glucose molecule from C-4 and C-3' of MulA, respectively. Our speculation on the structures of the two monoglucosides was supported by an acidic hydrolytic study of MulA, which yielded, in addition to OXY, the same two monoglucosides as evidenced by UV and MS spectra and retention time data. The structures of the two metabolites were thereby speculated as OXY-3'-*O*- β -*D*-glucopyranoside and OXY-4-*O*- β -*D*-glucopyranoside, respectively. Zhaxi's group also reported two monoglucosides of OXY in rat feces and gut contents after an oral dosage of MulA; yet, the structures were determined to be

Table 2. ^1H and ^{13}C NMR Spectroscopic Data for Metabolite G4 and Oxyresveratrol


Position	δ_{C}	$\delta_{\text{H}}^{\text{a}}$	$\delta_{\text{C}}^{\text{b}}$	$\delta_{\text{H}}^{\text{b}}$
1	117.9		115.3	
2	157.4		156.0	
3	103.0	6.53 (1H, d, $J = 2.3$ Hz)	102.6	6.31 (1H, d, $J = 2.3$ Hz)
4	158.1		158.1	
5	109.9	6.47 (1H, dd, $J = 8.6, 2.3$ Hz)	107.2	6.23 (1H, dd, $J = 8.4, 2.3$ Hz)
6	126.7	7.47 (1H, d, $J = 8.5$ Hz)	127.2	7.33 (1H, d, $J = 8.4$ Hz)
α	122.4	7.31 (1H, d, $J = 16.5$ Hz)	123.2	7.14 (1H, d, $J = 16.4$ Hz)
β	126.1	6.80 (1H, d, $J = 16.5$ Hz)	124.6	6.76 (1H, d, $J = 16.4$ Hz)
1'	139.7		140.0	
2'	104.4	6.39 (1H, d, $J = 2.0$ Hz)	104.0	6.33 (1H, d, $J = 2.0$ Hz)
3'	158.4		158.5	
4'	101.6	6.10 (1H, d, $J = 2.0$ Hz)	101.4	6.06 (1H, t, $J = 2.0$ Hz)
5'	158.4		158.5	
6'	104.4	6.39 (1H, d, $J = 2.0$ Hz)	104.0	6.33 (1H, d, $J = 2.0$ Hz)
Glu-1 ^{''c}	100.6	4.95 (1H, d, $J = 8.0$ Hz)		
2''	73.2	3.3–3.5 (3H, n)		
3''	75.8			
4''	71.4			
5''	75.3	3.85 (1H, n)		
6''	170.0			

^aMeasured in DMSO-*d*₆. ^bCited from ref 11. ^cGlu is the glucuronosyl moiety.

OXY-3'-*O*- β -D-glucopyranoside and OXY-2'-*O*- β -D-glucopyranoside.¹¹ The discrepancy between our speculation from in vitro incubation and the previous in vivo study might be due to the occurrence of isomerization and warrants further study.

The present study also revealed an insignificant species difference between human and rat in intestinal bacterial conversion of MulA as judged from similar rapid elimination of MulA and the same three metabolites formed. This finding warrants the extrapolation of existing pharmacokinetic data obtained on rats to humans. The AUP values of the two monoglucoside of OXY indicated a slight regioselectivity in intestinal hydrolysis of C-4 and C-3' glucosides of MulA, although the position preference could not be determined in the present study. The two monoglucoside intermediates disappeared from the incubation system rapidly. Whether and how the two monoglucosides contribute to the health benefits of mulberry are unknown and warrant further study. In concert with a quicker elimination of MulA in human intestinal bacteria, OXY reached a plateau faster in human intestinal bacteria (2.5 vs 4 h with rat). Taken together, we can conclude that deglycosylation of MulA to form OXY in gut microbiota is rapid and should be of considerable importance in determining their systemic exposures and consequently respective contribution to benefits of mulberry in human body.

It has been reported that some phenolic aglycones permeated across the apical side of Caco-2 cell monolayers more easily than their glucosides.²⁴ In the present study, the bidirectional transport study on the Caco-2 model revealed low P_{app} values

($\times 10^{-7}$ cm s⁻¹) of MulA and high P_{app} ($\times 10^{-6}$ cm s⁻¹) of OXY, predicting a poor absorption (<20%) of MulA and a medium absorption (20 to ~70%) of OXY.²⁵ This much higher permeability of OXY, together with a rapid bacterial hydrolysis of MulA demonstrated in vitro, enables OXY as the main form that been absorbed after oral dosing of MulA or mulberry. This finding is in good agreement with the previous report that oral bioavailability of MulA in the rat was about 1% and OXY and its derivatives accounted for 50% of oral dose of MulA.¹⁰ The dose-independent permeation and comparable absorptive and secretory transports of MulA indicate a predominant passive diffusion, whereas P-gp and MRP(s) were demonstrated to be involved in OXY transport across Caco-2 cells (Table 1). The efflux-mediated property of OXY transport should arouse attentions on potential interactions during dietary or medicinal uses of OXY or mulberry-derived products. Interestingly, resveratrol, the polyhydroxystilbene that lacks the hydroxyl group at C-2 position when compared to OXY, is a substrate of MRP2²⁶ but not that of MRP1 and P-glycoprotein.²⁷ These findings suggest that the difference in number and position of hydroxyl substitution might be crucial for transepithelial permeability of *trans*-hydroxystilbenes. Moreover, although there was considerable resveratrol accumulation in Caco-2 cells,²⁸ the accumulation of OXY was insignificant. This might explain the absence of conjugation (glucuronidation or sulfation) of OXY, although conjugation of resveratrol (main sulfation and minor glucuronidation) was observed during their transport across Caco-2 cells.²⁹

Hepatic metabolic stability is another determinant factor for in vivo fates of many xenobiotics. In the present study, MulA was unaltered in human and rat liver preparations. In contrast, OXY underwent extensive phase II conversions (major glucuronidation and minor sulfation) in liver microsomes of both species, predicting a significant hepatic first-pass metabolism and similar pharmacokinetic profiles between humans and rats. These in vitro data were in line with previous in vivo findings that glucuronidated and sulfated OXY were mainly identified in rat plasma, urine, and bile samples after oral administration of MulA^{10,11} or OXY²⁰ and thereby warrant further investigational emphasis on contributions of OXY and its metabolites to mulberry benefits. More interestingly, there were four OXY monoglucuronidates formed in both HLMs and RLMs, corresponding to the four hydroxyl groups in OXY, but only one monosulfated product of OXY was detected in hepatic S9 of both species. Rat hepatic subcellular preparations exhibited slightly higher activities for OXY glucuronidation and sulfation than those of human. It was noteworthy that there was an apparent positional preference with hepatic glucuronidation of OXY, which varied with species. The major product G4 of HLMs was first identified as 2-glucuronosyl of OXY and accounted for around 93% of total OXY glucuronides formed by HLMs. Similar regioselective glucuronidation in HLMs has been identified with resveratrol.³⁰ The predominant metabolite G3 in RLMs accounted for about 85% of total glucuronides formed by RLMs; yet, the absolute structure remained to be determined. This distinct positional preference of OXY glucuronidation may result in different bioactivities in humans and rats, which warrant further study. Reaction phenotyping study and biological evaluation of OXY-2-O- β -D-glucuronosyl (G4) are ongoing in our laboratory.

AUTHOR INFORMATION

Corresponding Author

*Tel: 853-83974876. Fax: 853-28841358. E-mail: ruyan@umac.mo.

Funding

The present work is supported by the National Basic Research Program of China (973 program, 2009CB522707) and the Research Committee of the University of Macau [RG086/09-10S/YR/ICMS and MYRG162(Y1-L2)-ICMS11-YR].

ABBREVIATIONS USED

MulA, mulberroside A; OXY, oxyresveratrol; UV, ultraviolet; MS, mass spectrometry; NMR, nuclear magnetic resonance; NOESY, nuclear Overhauser effect spectroscopy

REFERENCES

- (1) The State Pharmacopoeia Commission of P. R. China. *Pharmacopoeia of People's Republic of China*; Chemical Industry Press: Beijing, China, 2010.
- (2) Naowaboot, J.; Pannangpetch, P.; Kukongviriyapan, V.; Kongyingyoes, B.; Kukongviriyapan, U. Antihyperglycemic, antioxidant and antiglycation activities of mulberry leaf extract in streptozotocin-induced chronic diabetic rats. *Plant Foods Hum. Nutr.* **2009**, *64*, 116–121.
- (3) Lee, Y. J.; Choi, D. H.; Kim, E. J.; Kim, H. Y.; Kwon, T. O.; Kang, D. G.; Lee, H. S. Hypotensive, hypolipidemic, and vascular protective effects of *Morus alba* L. in rats fed an atherogenic diet. *Am. J. Chin. Med.* **2011**, *39*, 39–52.
- (4) Chang, L. W.; Juang, L. J.; Wang, B. S.; Wang, M. Y.; Tai, H. M.; Hung, W. J.; Chen, Y. J.; Huang, M. H. Antioxidant and antityrosinase

activity of mulberry (*Morus alba* L.) twigs and root bark. *Food Chem. Toxicol.* **2011**, *49*, 785–790.

- (5) Katsube, T.; Yamasaki, M.; Shiwaku, K.; Ishijima, T.; Matsumoto, I.; Abe, K.; Yamasaki, Y. Effect of flavonol glycoside in mulberry (*Morus alba* L.) leaf on glucose metabolism and oxidative stress in liver in diet-induced obese mice. *J. Sci. Food. Agric.* **2010**, *90*, 2386–2392.
- (6) Asano, N.; Yamashita, T.; Yasuda, K.; Ikeda, K.; Kizu, H.; Kameda, Y.; Kato, A.; Nash, R. J. Polyhydroxylated alkaloids isolated from mulberry trees (*Morus alba* L.) and silkworms (*Bombyx mori* L.). *J. Agric. Food Chem.* **2001**, *49*, 4208–4213.
- (7) Piao, S. J.; Qu, G. X.; Qiu, F. Chemical constituents of the water extract from Mori Cortex. *Zhongguo Yaowu Huaxue Zazhi* **2006**, *16*, 40–45.
- (8) Wang, C. P.; Wang, Y.; Wang, X.; Zhang, X.; Ye, J. F.; Hu, L. S.; Kong, L. D. Mulberroside A possesses potent uricosuric and nephroprotective effects in hyperuricemic mice. *Planta Med.* **2011**, *77*, 786–794.
- (9) Kim, J. K.; Kim, M.; Cho, S. G.; Kim, M. K.; Kim, S. W.; Lim, Y. H. Biotransformation of mulberroside A from *Morus alba* results in enhancement of tyrosinase inhibition. *J. Ind. Microbiol. Biotechnol.* **2010**, *37*, 631–637.
- (10) Qiu, F.; Komatsu, K.; Saito, K.; Kawasaki, K.; Yao, X.; Kano, Y. Pharmacological properties of traditional medicines. XXII. Pharmacokinetic study of mulberroside A and its metabolites in rat. *Biol. Pharm. Bull.* **1996**, *19*, 1463–1467.
- (11) Zhaxi, M.; Chen, L.; Li, X.; Komatsu, K.; Yao, X.; Qiu, F. Three major metabolites of mulberroside A in rat intestinal contents and feces. *Planta Med.* **2010**, *76*, 362–364.
- (12) Wang, R. F.; Cao, W. W.; Cerniglia, C. E. PCR detection and quantitation of predominant anaerobic bacteria in human and animal fecal samples. *Appl. Environ. Microb.* **1996**, *62*, 1242–1247.
- (13) Blaut, M.; Clavel, T. Metabolic diversity of the intestinal microbiota: implications for health and disease. *J. Nutr.* **2007**, *137*, 751S–755S.
- (14) Turpeinen, M.; Ghiciuc, C.; Opritoui, M.; Tursas, L.; Pelkonen, O.; Pasanen, M. Predictive value of animal models for human cytochrome P450 (CYP) mediated metabolism: Comparative study in vitro. *Xenobiotica* **2007**, *37*, 1367–1377.
- (15) Liang, S. C.; Ge, G. B.; Liu, H. X.; Shang, H. T.; Wei, H.; Fang, Z. Z.; Zhu, L. L.; Mao, Y. X.; Yang, L. Determination of propofol UDP-glucuronosyltransferase (UGT) activities in hepatic microsomes from different species by UFLC-ESI-MS. *J. Pharm. Biomed.* **2011**, *54*, 236–241.
- (16) Lowry, O. H.; Rosebrough, N. J.; Farr, A. L.; Randall, R. J. Protein measurement with the Folin phenol reagent. *J. Biol. Chem.* **1951**, *193*, 265–275.
- (17) Ruan, J. Q.; Leong, W. I.; Yan, R.; Wang, Y. T. Characterization of metabolism and in vitro permeability study of notoginsenoside R1 from Radix Notoginseng. *J. Agric. Food Chem.* **2010**, *58*, 5770–5776.
- (18) Yan, R.; Ko, N. L.; Lin, G.; Tam, Y. K. Low oral bioavailability and pharmacokinetics of ligustilide, a major bioactive component in Rhizoma Chuanxiong, in the rat. *Drug Metab. Dispos.* **2008**, *36*, 400–408.
- (19) Voigt, W. Sulforhodamine B assay and chemosensitivity. *Methods Mol. Med.* **2005**, *110*, 39–48.
- (20) Huang, H.; Chen, G.; Lu, Z.; Zhang, J.; Guo, D. A. Identification of seven metabolites of oxyresveratrol in rat urine and bile using liquid chromatography/tandem mass spectrometry. *Biomed. Chromatogr.* **2010**, *24*, 426–432.
- (21) Chao, J.; Yu, M. S.; Ho, Y. S.; Wang, M.; Chang, R. C. Dietary oxyresveratrol prevents parkinsonian mimetic 6-hydroxydopamine neurotoxicity. *Free Radical Biol. Med.* **2008**, *45*, 1019–1026.
- (22) Lorenz, P.; Roychowdhury, S.; Engelmann, M.; Wolf, G.; Horn, T. F. Oxyresveratrol and resveratrol are potent antioxidants and free radical scavengers: Effect on nitrosative and oxidative stress derived from microglial cells. *Nitric Oxide-Biol. Chem.* **2003**, *9*, 64–76.
- (23) Kim, Y. M.; Yun, J.; Lee, C. K.; Lee, H.; Min, K. R.; Kim, Y. Oxyresveratrol and hydroxystilbene compounds. Inhibitory effect on

tyrosinase and mechanism of action. *J. Biol. Chem.* **2002**, *277*, 16340–16344.

(24) Liu, Y.; Hu, M. Absorption and metabolism of flavonoids in the caco-2 cell culture model and a perused rat intestinal model. *Drug Metab. Dispos.* **2002**, *30*, 370–377.

(25) Artursson, P.; Karlsson, J. Correlation between oral drug absorption in humans and apparent drug permeability coefficients in human intestinal epithelial (Caco-2) cells. *Biochem. Biophys. Res. Commun.* **1991**, *175*, 880–885.

(26) Henry, C.; Vitrac, X.; Decendit, A.; Ennamany, R.; Krisa, S.; Mérillon, J. M. Cellular uptake and efflux of trans-piceid and its aglycone trans-resveratrol on the apical membrane of human intestinal Caco-2 cells. *J. Agric. Food Chem.* **2005**, *53*, 798–803.

(27) Li, Y.; Revalde, J. L.; Reid, G.; Paxton, J. W. Interactions of dietary phytochemicals with ABC transporters: possible implications for drug disposition and multidrug resistance in cancer. *Drug Metab. Rev.* **2010**, *42*, 590–611.

(28) Maier-Salamon, A.; Hagenauer, B.; Wirth, M.; Gabor, F.; Szekeres, T.; Jäger, W. Increased transport of resveratrol across monolayers of the human intestinal Caco-2 cells is mediated by inhibition and saturation of metabolites. *Pharm. Res.—Dordr.* **2006**, *23*, 2107–2115.

(29) Sabolovic, N.; Humbert, A. C.; Radomska-Pandya, A.; Magdalou, J. Resveratrol is efficiently glucuronidated by UDP-glucuronosyltransferases in the human gastrointestinal tract and in Caco-2 cells. *Biopharm. Drug Dispos.* **2006**, *27*, 181–189.

(30) Aumont, V.; Krisa, S.; Battaglia, E.; Netter, P.; Richard, T.; Mérillon, J. M.; Magdalou, J.; Sabolovic, N. Regioselective and stereospecific glucuronidation of trans- and cis-resveratrol in human. *Arch. Biochem. Biophys.* **2001**, *393*, 281–289.